Nanomed. J., 4(2): 115-125, Spring 2017

ORIGINAL RESEARCH PAPER

Curcumin coated gold nanoparticles: synthesis, characterization, cytotoxicity, antioxidant activity and its comparison with citrate coated gold nanoparticles

Elnaz Shaabani [1], Seyed Mohammad Amini [1], Sharmin Kharrazi [1], Roksana Tajerian [2]*

[1] *Department of Medical Nanotechnology, School of Advanced Technologies in Medicine (SATiM), Tehran University of Medical Sciences (TUMS), Tehran, Iran*

[2] *Department of Tissue Engineering and Applied Cell Sciences, School of Advanced Technologies in Medicine (SATiM), Tehran University of Medical Sciences (TUMS), Tehran, Iran*

ABSTRACT

Objective(s): Biological applications of gold nanoparticles have limitations because of the toxic chemicals used in their synthesis. Curcumin can be used as reducing as well as capping agent in synthesis of GNPs to eliminate the cytotoxicity. Conjugation of curcumin to gold also helps in increasing its solubility and bioavailability.

Materials and Methods: Here we report synthesis of gold nanoparticles coated with citrate and curcumin and of two different sizes via chemical routes. UV-Vis absorbance spectroscopy, Dynamic Light Scattering and Transmission Electron Microscopy were applied to study the average particle size, size stability of the samples and zeta potential. Fourier transform infrared, Raman Spectroscopy and Fluorescence Spectroscopy were applied for detection of curcumin on the surface of GNPs. The antioxidant activity was evaluated using DPPH assay and Cytotoxicity was evaluated by MTT assay.

Results: Particles were synthesized of 6 and 16 nm size. The average particle size was found to be 21.7 ± 5.7 by TEM. The zeta potential on the surface of Cur-GNPs was negative and larger than 25 mV which is a sign of their high stability. The stability of these particles (with different coatings but with similar sizes) at different time intervals (up to 3 months) and also in different media like cell culture medium, different buffers, glucose and at different pH conditions have been investigated thoroughly. Appearance of functional groups assigned to curcumin in FTIR and SERS spectra are sign of presence of curcumin in the sample. The quenching of the fluorescence in the presence of GNPs reveals the clear indication of the capping and binding of curcumin with GNPs. Cur-GNP1 (16 nm) were found to exhibit highest antioxidant activity than other gold nanoparticles. Cytotoxicity evaluation using MTT assay on L929 cell line proved curcumin coated gold nanoparticles were non-toxic up to 40 ppm.

Conclusion: The results revealed that larger curcumin coated gold nanoparticles were stable and also non-toxic and were found suitable for further in-vitro and in-vivo studies.

Keywords: *Anti-oxidant activity, Curcumin, Gold nanoparticles, Green synthesis*

How to cite this article

Shaabani E, Amini SM, KharrazI Sh, Tajerian R. Curcumin coated gold nanoparticles: synthesis, characterization, cytotoxicity, antioxidant activity and its comparison with citrate coated gold nanoparticles. Nanomed J. 2017; 4(2): 115-125.
DOI:10.22038/nmj.2017.21506.1227

INTRODUCTION

Phenomenal properties of metal nanoparticles have fascinated scientists of various fields for over a century and yielded novel applications in medicine and engineering. Metal nanoparticles have attracted great attention because of their great potential in medical nanotechnology[1]. Among different kinds of metal nanoparticles, gold nanoparticles have great importance because of their unique properties like tunable surface plasmon resonance (SPR)[2],

*Corresponding Author Email: *sh-kharrazi@tums.ac.ir*
Tel: (+98) *2143052135*

Note. This manuscript was submitted on January 28, 2017; approved on February 12, 2017

biocompatibility, high surface reactivity, oxidation resistance and allocated promising therapeutic opportunities in nanomedicine[3].

Different synthesis methods such as chemical, physical and biological have been used for Gold nanoparticles (GNPs). Chemical methods are widely used for synthesis of metallic nanoparticles as they make it possible to control synthesis processes with high and fast performance [4, 5]. Chemical methods are often based on metal ions reduction in solution by reductive and capping agents such as sodium borohydride, sodium citrate and sodium dodecyl sulfate. Most of these materials are toxic and their use in medical research is restricted. In addition, some of these materials remain unreacted and free in solution and can end up as environmental pollution [6].

To overcome these drawbacks, in recent years biological or green chemistry synthesis methods has found more importance. "Biological synthesis" means the utilization of biological organisms like microorganisms in synthesis process, which consists of different species of bacteria, actinomycetes, algae, fungi, yeast and biomass or plant extracts [7]. Biological or green synthesis methods provide improvements over the physical and chemical methods. They are environment friendly, affordable, easy to scale-up for large scale synthesis and further there is no need to use high pressure, high energy, high temperature and toxic chemicals [8].Using plant extracts for synthesis of nanoparticles may be better than other biological methods because it eliminates the elaborate preservation of cell cultures, is suitable for large scale synthesis and also can be more affordable [9].

Biosynthesis of gold nanoparticles with extract/ broth of plants such as lemongrass [10] aloevera [11], tamarind leaf, tamarind [12], cumin seed [13], mirabilis jalapa flowers [14] and curcumin [15] have been reported in previous studies.

Curcumin is a polyphenol derived from turmeric plant that is widely used in food preparation and for medical purposes in south-east Asia, China and India. Investigations on the event of medical purposes for curcumin indicated its anticancer, antimicrobial, antioxidant, and anti-inflammatory properties [16]. In spite of therapeutic potential of curcumin, its usage is limited due to low water solubility and low bioavailability which is a major challenge. In order to increase the bioavailability of curcumin, different methods have been used. some of these methods involved encapsulation of curcumin in liposomes [17, 18] and loading curcumin in micelles [19]. However, low encapsulation efficiency, rapid leakage of water-soluble drugs in the presence of blood compo-nents and poor storage stability are potential challenges for the future research of curcumin encapsulated in liposomes. Drug loading and tricky loading processes of micelles, too need to be improved. Another method is coupling of curcumin to noble metal nanoparticles, such as gold. Conjugation of curcumin to nanoparticles particularly in aqueous media can increase its activity, half-life, stability and increased stability in proprietary and non-proprietary metabolic processes[20].

Gold nanoparticles can be synthesized through direct reduction of gold ions ($HAuCl_4$) using curcumin (in absence of other reducing or stabilizing agents) in aqueous phase, so that surface of gold nanoparticle is covered by curcumin [15, 21, 22]. Here, we report synthesis of curcumin coated gold nanoparticles of two different sizes through variation of curcumin content in the samples. These particles have been studied in comparison with chemically synthesized GNPs coated with citrate molecules for their stability, cytotoxicity (L929 cell line) and antioxidant activity.

MATERIALS AND METHODS

Materials

Tetra chloroauric (III) acid trihydrate ($HAuCl_4 \cdot 3H_2O$, 99.9%, Merck Chemicals, Germany), Curcumin ($C_{21}H_{20}O_6$, 65%, Sigma-Aldrich, USA), Dimethyl sulfoxide (DMSO) (C_2H_6OS, 99.5%, Sigma-Aldrich, USA), Potassium carbonate (K_2CO_3, 99%, Merck Chemicals, Germany), Sodium borohydride ($NaBH_4$, 98%, Merck Chemicals, Germany), Tri-Sodium citrate dehydrate ($C_6H_5Na_3O_7 \cdot 2H_2O$, 99%, Merck Chemicals, Germany), Diphenylpicrylhydrazyl (DPPH) ($C_{18}H_{12}N_5O_6$, Sigma-Aldrich, USA), Methanol (CH_3OH, 99.9%, Merck Chemicals, Germany), DMEM-F12 (GIBCO/BRL Invitrogen, Carlsbad, California), Fetal bovine serum (FBS) (GIBCO/BRL Invitrogen, Carlsbad, California), Trypsin (Biosera, England), Penicillin-Streptomycin (Biosera, England) and methylthiazolyl diphenyl-tetrazolium bromide (MTT, 98%, Sigma-Aldrich, USA) were all purchased and used without any further purification. All aqueous solutions were prepared with DI water (Barnsted E-PureTM 18.3 MΩ water).

Synthesis of Gold Nanoparticles coated with curcumin (Cur-GNPs)

For synthesis of gold nanoparticles 120 µl of 20 mM solution of curcumin in DMSO is initially added to 7 ml of DI water. The pH of this solution was set in the range of 9-10 by drop-wise addition of K_2CO_3 150 mM aqueous solution. This was allowed to stir for 5 min in order to let curcumin release its hydrogens of hydroxyl groups for reduction of Au ions. Finally 2.5 ml solution of $HAuCl_4$ (4 mM solution in water) was drop-wise added to the above solution and final volume was set to 10 ml by addition of DI water. After 4 h of vigorous stirring the reaction was completed. This colloidal solution was aged for 3 days in order to allow the reaction to get completed. Increasing the amount of curcumin resulted in formation of smaller particles. In order to wash off the un-reacted curcumin from the samples centrifuge filter tubes (Amicon Ultra-50 Centrifugal Filter Units, Merck, Germany) were used at 4000 rpm for 4 min (Eppendorf . . . . . °C). The centrifugation process was repeated for four times until no sign of curcumin in UV-Vis absorbance spectra was observed.

Synthesis of Gold nanoparticles coated with citrate (Cit-GNPs)

In order to compare the functionality of curcumin coated samples with un-coated samples, GNPs with citrate coating were synthesized. 0.5 ml of 0.04 M solution in water of tri sodium citrate was added to 10 ml of 0.5 mM aqueous $HAuCl_4$. After 15 min of stirring, 0.5 ml of 0.1 M fresh and ice cold aqueous solution of sodium borohydride was injected to the mixture. The reaction was stopped after 15 min. For synthesis of larger particles 0.02 M solution of tri sodium citrate and 0.5 mM solution of sodium borohydride were used.

UV-Vis absorbance Spectroscopy

UV-Vis absorbance spectroscopy was applied to study the average particle size and size stability of the samples (Bio Aquarius CE 7250, United Kingdom). The data reported by Haiss et al. was used for estimation of average size of gold nanoparticles [23].

Dynamic Light Scattering (DLS) measurements

The average particle size (hydrodynamic diameter), size distribution of the particle and the zeta potential were measured on Zeta sizer, Malvern Instruments Ltd., USA. Measurements were repeated three times and the results were reported as mean ±SD.

Transmission Electron Microscopy (TEM)

TEM was applied to study the morphology, size and size distribution of the synthesized particles. TEM micrographs were recorded using a Zeiss-EM10C-100 KV (Germany) electron microscope. The sample was drop-casted on a carbon coated copper grid and air dried for imaging.

Fourier transform infrared (FTIR) Spectroscopy

To determine the specific site of interaction of Au^{3+} on curcumin and the possible functional groups drawn in the formation of GNPs, FTIR has been performed. The Cur-GNPs were washed and freeze dried with Telstar freeze dryers Lyo Quest -85 (Spain) to obtain dry powder For FTIR measurements. The finely powdered samples were made in to pellets after mixing with KBr powder. Spectra were collected in a Nicolet iS10 spectrometer (USA) over a range of 4000 cm^{-1} to 400 cm^{-1}.

Raman Spectroscopy

Surface enhanced Raman scattering (SERS) signals were collected with a portable Raman spectrometer (Avantes AvaSpec-ULS2048XL, Netherlands) in order to study the functional groups on the surface of particles.

Fluorescence Spectroscopy

Fluorescence measurements were carried out using a Varian Cary Eclipse fluorescence spectrophotometer (Varian Scientific Instruments, Mulgrave, Australia). The emission spectra were recorded from 450 nm to 900 nm at an excitation wavelength of 420 nm. The slit width was 10 nm for both excitation and emission.

DPPH Radical Scavenging Assay

The antioxidant capacity of the samples was measured using the DPPH assay [24]. DPPH is a stable, purple colored free radical which turns yellow (the stable non-radical compound 1,1-diphenyl-2-picril-hydrazine) when scavenged. This property of the radical is exploited to exhibit the antioxidant activity of the GNPs. In each micro-tube, 1 ml DPPH 0.1 mM solution in methanol was mixed with 1 ml

different concentration of gold nanoparticle solutions (156 ppm- 1.56 ppm) diluted in methanol. The absorbance was measured at 517nm using Bio Aquarius CE 7250 (United Kingdom). The absorbance of the sample solution was used to calculate the inhibition percentage via the equation below:

$$\text{Inhibition percentage of DPPH} = \frac{(\text{absorbance of control solution} - \text{absorbance of sample}^{*})}{\text{absorbance of control solution}} \times 100 \quad (1)$$

*Absorbance of GNPs was recorded at 517 nm for correction.

Higher the inhibition percentage, stronger the antioxidant activity of the samples.

In vitro Cytotoxicity Evaluation of GNPs

The cytotoxicity of GNPs on fibroblast L929 cells was determined by MTT assay [25]. Cells were maintained at 37 °C under 5% CO_2 in DMEM-F12 with 10% fetal bovine serum and 1% penicillin/ streptomycin. After adequate growth, the cells were trypsinized and 1×10^4 cells/well were seeded in three 96-well cell culture plates. Each well contained 100 µl of cell suspension and the plates were incubated for 24 h at 37 °C under 5% CO_2 to obtain a monolayer cell. After that, the old media was removed from each well and the cells were categorized as control (untreated), treated-1 (treated with different concentrations of Cur-GNP1), treated-2 (treated with different concentrations of Cur-GNP2), treated-3 (treated with different concentrations of Cit-GNP1) and treated-4 (treated with different concentrations of Cit-GNP2). 100 µL of 2X media plus 100 µL 0f GNPs were added per well.

The experiments were repeated in triplicate. Following a 24, 48, 72 h incubation period at 37 °C under 5% CO_2, cell viability of plates was assessed. 20 ìL of MTT solution in PBS (5 mg/mL) was added to each well and incubated for 4 h in dark. Afterwards the supernatant was discarded and formazan crystals were dissolved in 100 µL DMSO and were shook to ensure complete dissolution of the formazan precipitate. ELx800 Absorbance Microplate Reader (Biotek, United States) was used to measure the optical density at 570 nm. The level of cytotoxicity was calculated via the equation below:

$$\text{Cell viability \%} = \frac{\text{Optical density(OD) in sample well}}{\text{optical density(OD) in control well}} \times 100$$

RESULTS AND DISCUSSION

Synthesis and Characterization of GNPs

For the synthesis of Curcumin coated GNPs, it was necessary to dissolve curcumin in dimethyl sulfoxide (DMSO) and its further dilution with water was possible at elevated pH. By increasing pH, from 5 to 9, absorbance spectra of curcumin showed a red shift as a result of de-protonation of curcumin (Fig. 1a). Increasing pH of curcumin is necessary for releasing hydrogens of its hydroxyl groups for reduction of Au ions. Addition of $HAuCl_4$ must not happen later than 5 min because after 5 min at this pH of 9 curcumin started degrading (Fig. 1b) [26, 27].

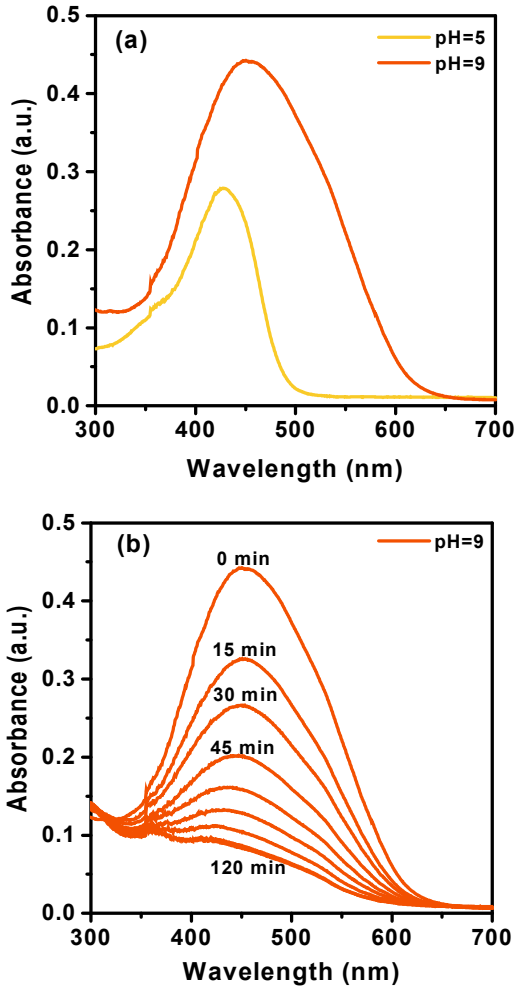

Fig. 1. (a) The UV-Vis absorbance spectra of 2×10^{-5}M curcumin in 1:1 methanol/H_2O at two different pH. (b) Kinetics of degradation of curcumin at pH=9

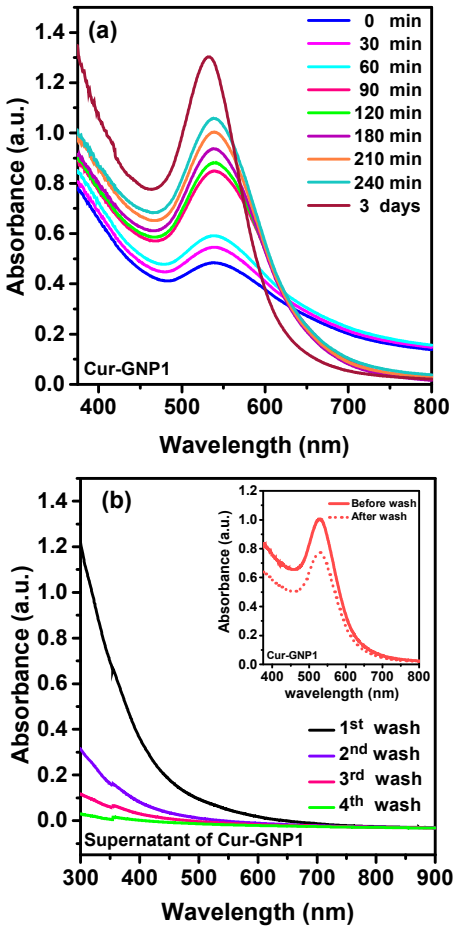

Fig. 2. (a) Kinetics of Cur-GNP1 formation (b) UV-Vis absorbance spectra of Cur-GNP1 supernatant after every step of washing and the spectra of Cur-GNP after and before washing (inset)

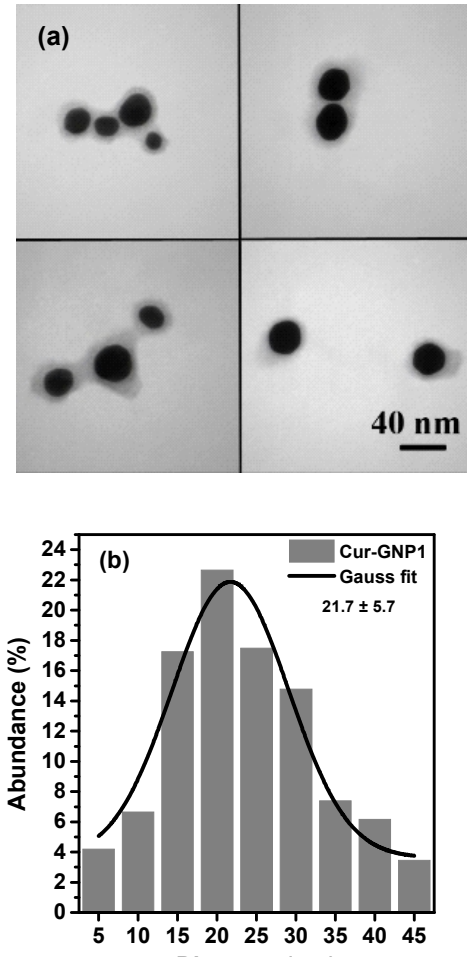

Fig. 3. (a) TEM micrographs of Cur-GNP1 and (b) corresponding size distribution histogram

In order to remove un-reacted curcumin from the samples, Cur-GNPs were washed and the absorbance spectra of the supernatant were checked after each step of centrifugation. After fourth time washing, absorbance spectrum of supernatant showed no sign of un-reacted curcumin or $HAuCl_4$ (Fig. 2b). After washing, the intensity of SPR slightly decreased because of removing curcumin which has an absorbance peak around 428 nm (Fig. 2b).

TEM micrographs confirmed formation of nanoparticles, and also indicated that the particles were faceted (Fig. 3a). The average particle size was found to be 21.7 ± 5.7 nm by measuring the size of more than 400 particles (Fig. 3b).

The citrate stabilized particles were synthesized in two different sizes as explained before.

UV-Vis absorbance spectra of curcumin and citrate coated gold nanoparticles of two sizes are presented in Fig.4 average particle size was estimated for all samples based on their UV-Vis absorbance spectra (Table 1).

Dynamic light scattering (DLS) was applied to measure the hydrodynamic diameter of the particles. Adding more curcumin/citrate during the synthesis of gold nanoparticles lead to formation of smaller particles thus the total surface area increased, allowing presence of/accommodating more number of curcumin /citrate molecules and hence resulted in larger zeta potential.

The hydrodynamic size of GNPs was larger than their average particle size estimated based on UV-Vis spectra which is because of presence of curcumin

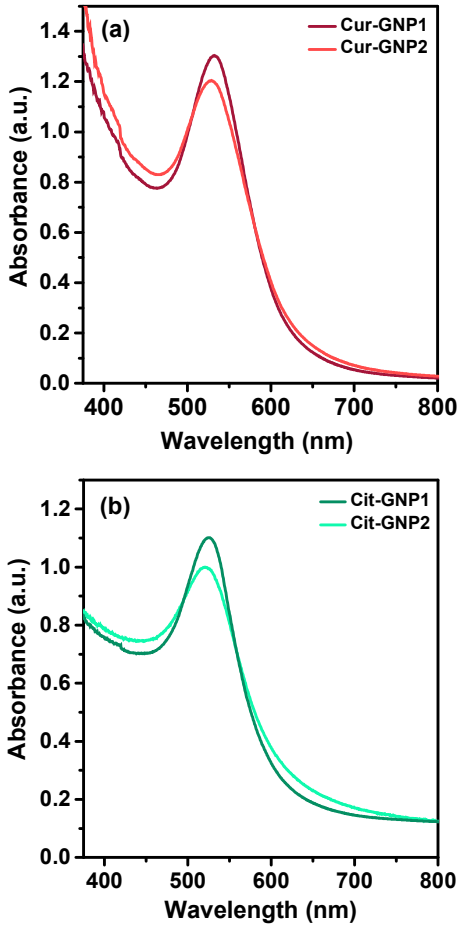

Fig. 4. UV-Vis absorbance spectra of (a) Cur-GNPs. (b) Cit-GNPs

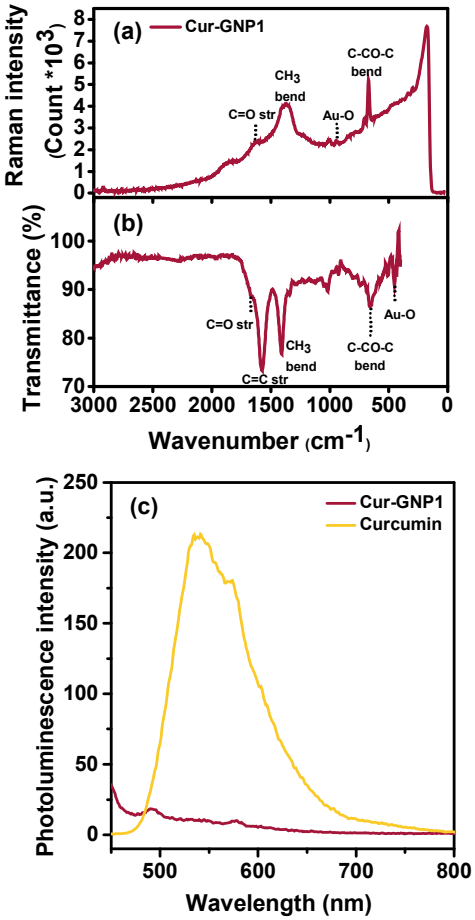

Fig. 5. (a) Raman spectrum (b) FTIR spectrum of Cur-GNP1 and (c) Fluorescence spectra of curcumin in 1:1 methanol/H_2O and Cur-GNP1

and citrate molecules on the surface of particles. The average hydrodynamic diameter of cur-GNPs did not change after washing, which is a sign of strong attachment of curcumin molecules to the surface of GNPs.

However after washing of Cur-GNPs, zeta potential decreased because of loss of some of unreacted curcumin around particles.

To investigate the presence of curcumin on the surface of GNPs, Gold nanoparticles made it possible to take advantage of Raman spectroscopy for surface enhance Raman scattering (SERS). The SERS and FTIR transmittance spectra of Cur-GNP1 are presented in Fig. 5a,b. As shown in the figure, the bands assigned to C=C and C=O stretching, CH_3 bending and C-CO-C bending are sign of presence of curcumin in the sample.

However C=O band shifted to smaller wave numbers in comparison with curcumin confirming that oxygen of C=O groups were coordinated to Au. After reaction with Au, a new band at ~ 450 cm^{-1} occurred in the FTIR spectrum of Cur-GNP1 which was absent in the spectrum of curcumin. This peak has been attributed to Me-O where metal complexes of curcumin have been investigated [28, 29].

However, the band at ~ 940 cm^{-1} in the Raman spectrum could also be attributed to Me-O as noted by Bich et al [30]. These data revealed the interaction between Au and oxygen atoms of C=O groups of curcumin.

Further, fluorescence spectra (photolumine-scence) of curcumin and Cur-GNPs were compared.

Table 1. Synthesis parameters, average particle size and zeta potential of different sample

Samples	Concentration of precursors (mM)				UV-Vis	DLS	
	$HAuCl_4$	Curcumin	$NaBH_4$	Sodium citrate	Average size (nm)	Average size (nm)	Zeta potential (mV)
Cur-GNP1	1	0.28	-	-	14.3	32.7± 2.9	-28.4 ± 1.0
Cur-GNP2	1	0.32	-	-	5.6	16.2 ± 0.4	-36.2 ± 2.2
Cur-GNP1 washed	1	0.28	-	-	15.6	29.7 ± 1.0	-22.2 ± 1.5
Cur-GNP2 washed	1	0.32	-	-	6.1	15.8 ± 0.0	-27.9 ± 0.1
Cit-GNP1	0.5	-	1.2	20	16.1	39.9 ± 1.7	-22.9 ± 5.6
Cit-GNP2	0.5	-	100	40	5.3	20.4 ± 2.6	-30.7 ± 1.5

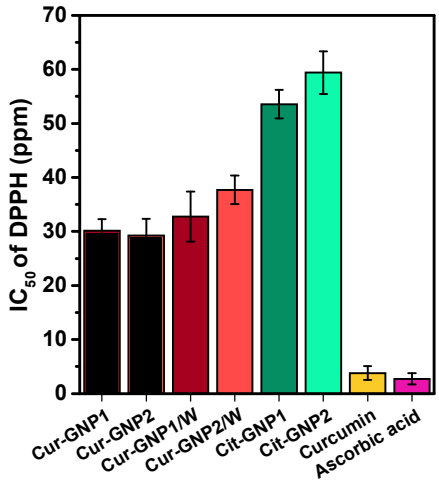

Fig. 6. DPPH inhibition (antioxidant activity) of GNPs and curcumin. (IC_{50} means the amount of material that can inhibit 50 present of DPPH free radical.)

Solution of curcumin in 1:1 methanol:H_2O was excited at the wavelength of 420 nm, its emission spectrum had a peak around 550 nm which matches the absorbance (SPR) peak of Cur-GNPs and thus get absorbed and the emission spectrum gets quenched in presence of Gold nanoparticles [31]. When reducing gold ions with curcumin, the oxidized curcumin molecules on the GNPs surface interact electronically with the surface to donate electron to the metal, thus quenching the fluorescence by non-radiative pathways available in the metal nanoparticles. The quenching of the fluorescence in the presence of GNPs reveals the clear indication of the capping and binding phenomenon of curcumin with GNPs (Fig. 5c).

Evaluation of Radical Scavenging Activity (DPPH assay)

The antioxidant activity of curcumin and GNPs synthesized by curcumin and $NaBH_4$ were determined using DPPH assay. Due to the inherent problems associated with measuring absolute solubility of curcumin in water, curcumin was dissolved in 1:1 methanol/H_2O.

The antioxidant properties of samples showed that the antioxidant activity of GNPs synthesized by curcumin was progressively higher than GNPs synthesized by $NaBH_4$ (Fig.6). Comparison of antioxidant properties of Cur-GNPs-washed, Cur-

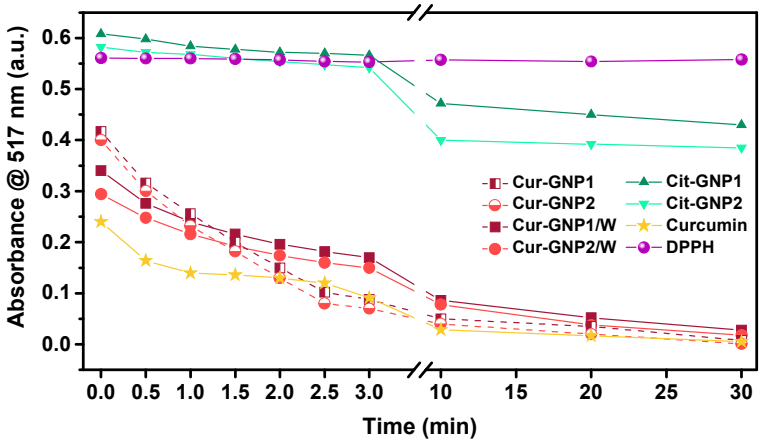

Fig. 7. Time variation of DPPH absorbance in presence of GNPs and curcumin in 1:1 methanol/H_2O

GNPs, Cit-GNPs and curcumin by passing time (time intervals of 30 seconds and later every 10 minutes), showed that antioxidant properties of Cur-GNPs and curcumin remained higher in contrast with Cit-GNPs. Curcumin has inherent antioxidant property, which increased in presence of GNPs (Fig.7). The antioxidant activity of washed samples decreased slightly because of removing un-bound curcumin from the solution.

Stability studies of GNPs

The SPR spectra of GNPs in DI water were monitored up to 3 months. Absorbance spectra of Cur-GNPs and Cit-GNPs (Fig. 8a, b) did not show any clear change which is a good sign that particles remained stable during that period.

Gold nanoparticles were dispersed in cell culture medium RPMI, different buffers, glucose and at different pH conditions at a ratio of 1:4 and UV–Vis absorbance spectra of the samples were recorded to monitor the stability of the nanoparticles. When particles were exposed to pH variation or addition of NaCl, Cit-GNPs exhibited better stability than Cur-GNPs, however both samples remained stable (Fig. 8c, d). The absorbance spectra of Cur-GNPs did not show a clear change when exposed to different media except

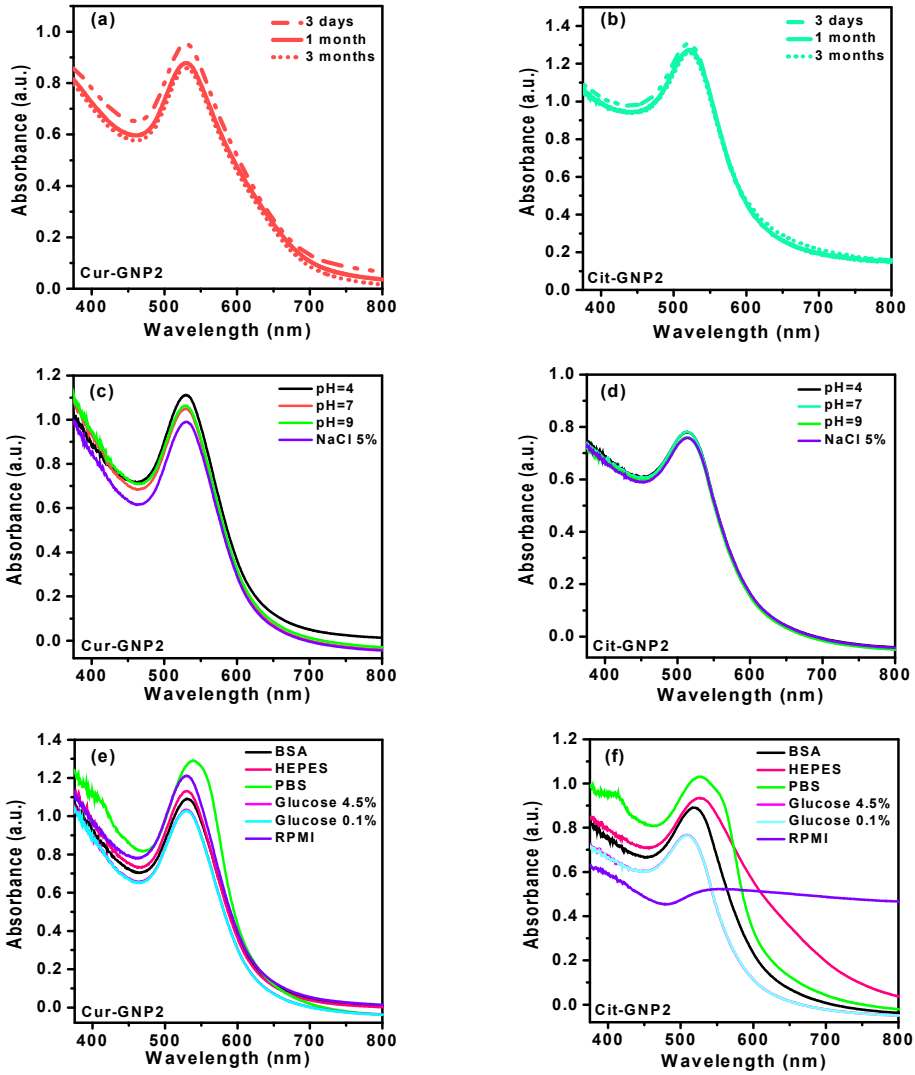

Fig. 8. Stability of GNPs. UV-Vis absorbance spectra of (a) Cur-GNP2 up to 3 month. (b) Cit-GNP2 up to 3 month. (c) Cur-GNP2 at different pH and suspended in NaCl 5%. (d) Cit-GNP2 suspended in different pH and NaCl 5%. (e) Cur-GNP2 suspended in

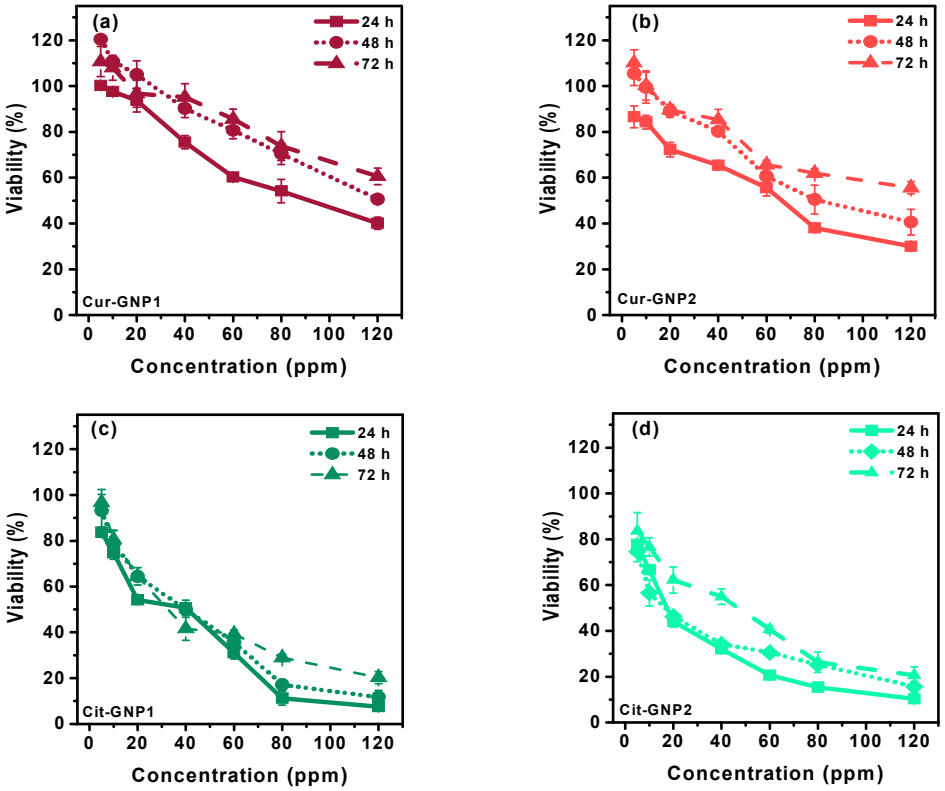

Fig. 9. In vitro cytotoxicity of Cur-GNPs and Cit-GNPs at different concentration on L929 cell line. (a) Cur-GNP1 (b) Cur-GNP2 (c) Cit-GNP1 (d) Cit-GNP2

for PBS which contains lots of ions and these might be the main cause of shift in SPR position (Fig. 8e).

However in case of Cit-GNPs, RPMI, HEPES and PBS caused noticeable change in the spectra which is greatly attributed to electrostatic coverage (loose bond) of citrate molecules (Fig. 8f). This difference in stability is mainly caused by the different coatings of GNPs.

Stability studies of GNPs

The SPR spectra of GNPs in DI water were monitored up to 3 months. Absorbance spectra of Cur-GNPs and Cit-GNPs (Fig. 8a, b) did not show any clear change which is a good sign that particles remained stable during that period.

Gold nanoparticles were dispersed in cell culture medium RPMI, different buffers, glucose and at different pH conditions at a ratio of 1:4 and UV–Vis absorbance spectra of the samples were recorded to monitor the stability of the nanoparticles. When particles were exposed to pH variation or addition of NaCl, Cit-GNPs exhibited better stability than Cur-GNPs, however both samples remained stable (Fig. 8c, d). The absorbance spectra of Cur-GNPs did not show a clear change when exposed to different media except for PBS which contains lots of ions and these might be the main cause of shift in SPR position (Fig. 8e).

However in case of Cit-GNPs, RPMI, HEPES and PBS caused noticeable change in the spectra which is greatly attributed to electrostatic coverage (loose bond) of citrate molecules (Fig. 8f). This difference in stability is mainly caused by the different coatings of GNPs.

Evaluation of Cytotoxicity (MTT assay)

In order to evaluate the cytotoxicity of the nanoparticles, *in vitro* cytotoxicity assay was performed on L929 cell line. The examination was performed at 3 time intervals (24, 48 and 72 h) and cells were treated with 8 sets of concentrations (Fig. 9). Viability of cells was evaluated based on equation 2. The data revealed that all nanoparticles were

nontoxic at concentrations up to 10 ppm. However particles remain show some toxicity at concentrations above 10 ppm. Cur-GNPs exhibit lower toxicity than Cit-GNPs.

CONCLUSION

Here, two different sizes of gold nanoparticle with two different coatings were synthesized. UV-Vis absorbance spectroscopy revealed that average size of particles was ~ 6 and 16 nm. The zeta potential on the surface of washed and un-washed was more than -25 mV which is a sign of their high stability. Cur-GNPs showed better stability in different buffer and different media than Cit-GNPs.

DPPH assay of particles revealed that washed and un-washed Cur-GNPs had great antioxidant activity which was better than GNPs alone. The curcumin coated GNPs were also found non-toxic on L929 cell line which makes them suitable for biological applications. However, it might be more convenient to use washed samples to make sure that no free curcumin is present in the solution.

ACKNOWLEDGMENTS

Authors wish to thank Ms. Mona Navaei-Nigjeh and Ms. Roya Karimi for their help.

CONFIICT OF INTEREST

The authors declare that there are no conflicts of interest.

REFERENCES

1. Mody, V.V., R. Siwale, A. Singh and H.R. Mody, Introduction to metallic nanoparticles. J Pharm Bioallied Sci. 2010; 2(4): 282.
2. Burke, T.R., B. Ye, X. Yan, S. Wang, Z. Jia, L. Chen, Z.-Y. Zhang and D. Barford, Small molecule interactions with protein-tyrosine phosphatase PTP1B and their use in inhibitor design. Biochemistry. 1996; 35(50): 15989-15996.
3. Guo, R., Y. Song, G. Wang and R.W. Murray, Does core size matter in the kinetics of ligand exchanges of monolayer-protected Au clusters. J Am Chem Soc. 2005; 127(8): 2752-2757.
4. Ackerson, C.J., P.D. Jadzinsky, J.Z. Sexton, D.A. Bushnell and R.D. Kornberg, Synthesis and bioconjugation of 2 and 3 nm-diameter gold nanoparticles. Bioconjug Chem. 2010; 21(2): 214-218.
5. Biswal, J., S. Ramnani, S. Shirolikar and S. Sabharwal, Synthesis of rectangular plate like gold nanoparticles by in situ generation of seeds by combining both radiation and chemical methods. Radiat Phys Chem. 2011; 80(1): 44-49.
6. Noruzi, M., D. Zare, K. Khoshnevisan and D. Davoodi, Rapid green synthesis of gold nanoparticles using Rosa hybrida petal extract at room temperature. Spectrochim Acta A Mol Biomol Spectrosc. 2011; 79(5): 1461-1465.
7. Nath, D. and P. Banerjee, Green nanotechnology–A new hope for medical biology. Environ Toxicol Pharmacol. 2013; 36(3): 997-1014.
8. Mohanpuria, P., N.K. Rana and S.K. Yadav, Biosynthesis of nanoparticles: technological concepts and future applications. J Nanopart Res. 2008; 10(3): 507-517.
9. Sathishkumar, M., K. Sneha, S. Won, C.-W. Cho, S. Kim and Y.-S. Yun, Cinnamon zeylanicum bark extract and powder mediated green synthesis of nano-crystalline silver particles and its bactericidal activity. Colloids Surf B Biointerfaces. 2009; 73(2): 332-338.
10. Shankar, S.S., A. Rai, B. Ankamwar, A. Singh, A. Ahmad and M. Sastry, Biological synthesis of triangular gold nanoprisms. Nat Mater. 2004; 3(7): 482-488.
11. Chandran, S.P., M. Chaudhary, R. Pasricha, A. Ahmad and M. Sastry, Synthesis of gold nanotriangles and silver nanoparticles using Aloevera plant extract. Biotechnol Prog. 2006; 22(2): 577-583.
12. Ankamwar, B., M. Chaudhary and M. Sastry, Gold nanotriangles biologically synthesized using tamarind leaf extract and potential application in vapor sensing. S Synth React Inorg Met Org Chem. 2005; 35(1): 19-26.
13. Sneha, K., M. Sathishkumar, S.Y. Lee, M.A. Bae and Y.-S. Yun, Biosynthesis of Au nanoparticles using cumin seed powder extract. J Nanosci Nanotechnol. 2011; 11(2): 1811-1814.
14. Vankar, P.S. and D. Bajpai, Preparation of gold nanoparticles from Mirabilis jalapa flowers. Indian J Biochem Biophys. 2010; 47(3): 157.
15. Singh, D.K., R. Jagannathan, P. Khandelwal, P.M. Abraham and P. Poddar, In situ synthesis and surface functionalization of gold nanoparticles with curcumin and their antioxidant properties: an experimental and density functional theory investigation. Nanoscale. 2013; 5(5): 1882-1893.
16. Lee, W.-H., C.-Y. Loo, M. Bebawy, F. Luk, R.S. Mason and R. Rohanizadeh, Curcumin and its derivatives: their application in neuropharmacology and neuroscience in the 21st century. Curr Neuropharmacol. 2013; 11(4): 338.
17. Agashe, H., K. Sahoo, P. Lagisetty and V. Awasthi, Cyclodextrin-mediated entrapment of curcuminoid 4-[3, 5-bis (2-chlorobenzylidene-4-oxo-piperidine-1-yl)-4-oxo-2-butenoic acid] or CLEFMA in liposomes for treatment of xenograft lung tumor in rats. Colloids Surf B Biointerfaces. 2011; 84(2): 329-337.
18. Mohanty, C., M. Das and S.K. Sahoo, Emerging role of nanocarriers to increase the solubility and bioavailability of curcumin. Expert Opin Drug Deliv. 2012; 9(11): 1347-1364.
19. Mohanty, C., S. Acharya, A.K. Mohanty, F. Dilnawaz and S.K. Sahoo, Curcumin-encapsulated MePEG/PCL diblock copolymeric micelles: a novel controlled delivery vehicle for cancer therapy. Nanomed. 2010; 5(3): 433-449.
20. Sindhu, K., R. Indra, A. Rajaram, K. Sreeram and R. Rajaram, Investigations on the Interaction of Gold–Curcumin Nanoparticles with Human Peripheral Blood Lymphocytes. J Biomed Nanotechnol. 2011; 7(1): 56-56.
21. Sreelakshmi, C., N. Goel, K. Datta, A. Addlagatta, R. Ummanni and B. Reddy, Green synthesis of curcumin capped gold

nanoparticles and evaluation of their cytotoxicity. Nanosci Nanotechnol Lett. 2013; 5(12): 1258-1265.
22. Sindhu, K., A. Rajaram, K. Sreeram and R. Rajaram, Curcumin conjugated gold nanoparticle synthesis and its biocompatibility. RSC Adv. 2014; 4(4): 1808-1818.
23. Haiss, W., N.T. Thanh, J. Aveyard and D.G. Fernig, Determination of size and concentration of gold nanoparticles from UV-vis spectra. Anal Chem. 2007; 79(11): 4215-4221.
24. Brand-Williams, W., M.-E Cuvelier and C. Berset, Use of a free radical method to evaluate antioxidant activity. LWT- Food Sci Technol. 1995; 28(1): 25-30.
25. Mosmann, T., Rapid colorimetric assay for cellular growth and survival: application to proliferation and cytotoxicity assays. J Immunol Methods. 1983; 65(1-2): 55-63.
26. Priyadarsini, K.I., Photophysics, photochemistry and photobiology of curcumin: Studies from organic solutions, bio-mimetics and living cells. J Photochem Photobiol C. 2009; 10(2): 81-95.
27. Wang, Y.-J., M.-H. Pan, A.-L. Cheng, L.-I. Lin, Y.-S. Ho, C.-Y. Hsieh and J.-K. Lin, Stability of curcumin in buffer solutions and characterization of its degradation products. J Pharm Biomed Anal. 1997; 15(12): 1867-1876.
28. Krishnankutty, K. and P. Venugopalan, Metal chelates of curcuminoids. Synth React Inorg Met Org Chem. 1998; 28(8): 1313-1325.
29. Xue, X., J. Wang, G. Si, C. Wang and S. Zhou, Synthesis, DNA-binding properties and cytotoxicity evaluation of two copper (II) complexes based on curcumin. Tranit Metal Chem. 2016; 41(3): 331-337.
30. Bich, V.T., N.T. Thuy, N.T. Binh, N.T.M. Huong, P.N.D. Yen and T.T. Luong, Structural and spectral properties of curcumin and metal-curcumin complex derived from turmeric (Curcuma longa), in Physics and Engineering of New Materials. 2009; Springer. 271-278.
31. Mooradian, A., Photoluminescence of metals. Phys Rev Lett. 1969; 22(5): 185.